

Optical-absorption spectra of inorganic fullerene-like MS_2 ($M=Mo, W$)

G. L. Frey

Department of Materials and Interfaces, Weizmann Institute, Rehovot 76100, Israel

S. Elani

The Racah Institute of Physics, The Hebrew University, Jerusalem 91904, Israel

M. Homyonfer, Y. Feldman, and R. Tenne

Department of Materials and Interfaces, Weizmann Institute, Rehovot 76100, Israel

(Received 8 May 1997; revised manuscript received 23 September 1997)

Optical-absorption spectroscopy of inorganic fullerene-like MoS_2 and WS_2 (IF- MoS_2 and IF- WS_2) is reported in the range 400–800 nm, at temperatures between 4–300 K, and compared to the corresponding bulk (2H) material. A systematic study of the effect of IF size and number of atomic layers on the optical properties shows that the semiconductivity of the layered material is preserved in the IF structures. Nevertheless, all IF with number of layers (n) > 6 exhibit a decrease in the A and B exciton energies. This redshift becomes larger as additional inner layers are formed, until a saturation value is reached ($n > 10$). We assign this redshift to the deformations, curvature, and discommensuration between adjacent atomic layers the structure must accommodate in order to form an IF structure. An increase in the exciton energies is observed in IF consisting of a few sulfide layers ($n < 5$). This blueshift is attributed to a quantum confinement in the z direction. Band-structure calculations show that an expansion of >7% along the c axis leads to a convergence of the levels K_1 and K_4 , which is displayed in the absorption spectra of IF with 1 or 2 layers. [S0163-1829(98)03111-7]

INTRODUCTION

In analogy to graphite nanoclusters, it was suggested that the abundance of dangling bonds on the periphery of layered metal dichalcogenides MX_2 (where $M=Mo, W$; $X=S, Se$) nanoparticles destabilize their planar topology. This instability was utilized for the synthesis of hollow cage structures of MX_2 , including nested polyhedra, nanotubes and structures with negative curvature, generically called *inorganic fullerene-like material*^{1,2} (IF) (see Fig. 1). Subsequently, the large-scale synthesis of IF- MS_2 ($M=Mo, W$) powder has been reported.^{3–5} The IF of metal dichalcogenides exhibit a variety of sizes and shapes and have been investigated by x-ray powder diffraction (XRD),³ scanning tunneling microscopy⁶ (STM), and high-resolution transmission electron microscopy (TEM).^{3–5} The present work is the study of the optical properties of these materials.

The physical and structural properties of crystalline transition-metal dichalcogenides are reviewed by Wilson and Yoffe.⁷ Electronic band-structure calculations were performed for 2H- MX_2 ($M=Mo, W$; $X=S, Se$) and are reviewed by Doni and Girlanda.⁸ The present status of experimental evidence appears to favor the model proposed by Coehoorn and co-workers.^{9,10} They found that the lowest allowed transition is indirect and the two higher excitonic transitions occur at the K point of the Brillouin zone. The optical transition in 2H- MoS_2 and 2H- WS_2 are summarized in Table I. The A and B excitons are assigned to transitions at the K point of the Brillouin zone, with K_4 and K_1 being the initial states, and K_5 the final state.¹⁰ The A and B splitting (K_4 and K_1) is due to interlayer interaction and spin-orbit splitting. The splitting values are 0.18 and 0.41 eV for 2H- MoS_2 and 2H- WS_2 , respectively.

Quantum confinement of carriers was also studied in transition-metal dichalcogenides. Their characteristic layered structure leads to a quantization effect in the c axis (perpendicular to the layers) in ultrathin platelets^{14–16} and to a quantum size effect in nanoparticles <45 Å.^{17,18}

This paper presents a comprehensive study of the optical properties of IF- MS_2 materials. The optical-absorption measurements show that the semiconductivity of MS_2 is preserved in the IF structure. Nevertheless, the position of the A and B excitons are altered in comparison to the 2H bulk. A systematic study of the effect of IF size and number of atomic layers reveals that the position of the excitons is dependent on the number of IF layers (n) rather than the particle size. All samples consisting of IF with $n > 6$ exhibit a redshift of the exciton energies, while all samples consisting of IF with $n < 5$ exhibit a blueshift of the exciton energies. This paper contains the experimental results and a statistical analysis in order to estimate the error introduced to the spectra due to sample inhomogeneity. In the discussion we argue the origins of the blueshift and the somewhat surprising red-

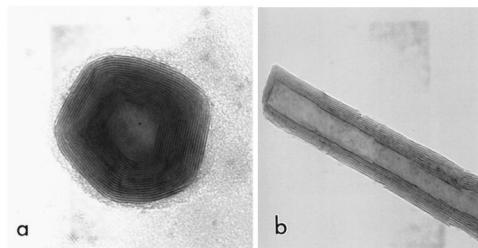


FIG. 1. TEM micrograph of (a) typical IF- MoS_2 particle, (b) typical WS_2 nanotube. The distance between two fringes (MS_2 layers) is 6.2 Å.

TABLE I. Optical transitions in 2H-MoS₂ and 2H-Ws₂ at various temperatures.

Material	Temp. (K)	Indirect band gap (eV)	Direct band gap (eV)	A exciton position (eV)	B exciton position (eV)
2H-MoS ₂	300	1.2 ^a	1.95 ^b	1.88 ^c	2.06 ^c
	150			1.90	2.10
	75			1.91	2.11
	25			1.91	2.11
2H-Ws ₂	300	1.3 ^d	2.05 ^d	1.95 ^d	2.36 ^d
	150			2.10	2.40
	75			2.05	2.45
	25			2.05	2.45

^aRoom-temperature values corresponding to those of Ref. 10.

^bRoom-temperature values corresponding to those of Ref. 12.

^cRoom-temperature values corresponding to those of Ref. 13.

^dRoom-temperature values corresponding to those of Ref. 11.

shift. We also present band-structure calculations that demonstrate the effect of the IF *c*-axis expansion on the optical properties.

EXPERIMENT

IF-MoS₂ and IF-Ws₂ were prepared from the respective oxide precursor following published procedures^{3–5} and were fully characterized by XRD and TEM. The proposed IF growth mechanism⁴ consists of the reaction between H₂S gas and the top surface of the oxide nanoparticle (<150 nm) so that a closed single or double MS₂ layer is produced within a few seconds. The sulfide layer prohibits fusion of the nanoparticles, and consequently the size of the IF particle is determined by the size of the incipient oxide nanoparticle. Simultaneously, the reducing atmosphere leads to partial reduction of the oxide core into MoO₂ or W₂₀O₅₈ (W₁₈O₄₉) within a few minutes. The oxide core is progressively converted into the respective IF within 30–90 min of annealing in H₂S atmosphere. This procedure permits a very good control over the number of MS₂ layers in the IF structure and somewhat lesser control over the size distribution of the nanoparticles. Alkali-doped suboxide precursors were also used and resulted in alkali intercalated IF-Ws₂ after sulfidization, which formed a stage-6 superlattice, and were soluble in alcoholic suspensions.⁵ The concentration of the alkali metal did not exceed a few percent (<5%) and therefore is not likely to affect the absorption spectra.¹³ Films (<2000 Å thick) consisting of IF with diameters in the range of 150–1500 Å were prepared according to published procedures on either quartz substrates^{3,4} or tin-doped indium oxide films.⁵

XRD (Ref. 4) and Raman¹⁹ analysis revealed that the 2H structure of the unit cell is locally preserved within an IF particle. Nonetheless, a shift of the XRD (0002) peak of the IF phase indicates a lattice expansion of ~2% between two adjacent MS₂ slabs along the *c* axis compared to the bulk 2H polytype. This expansion is attributed to the strain in the bent layers and to discommensuration between layers of different radii, i.e., different number of atoms.²⁰ Moreover, XRD and Raman measurements indicate that the *a* and *b* crystallo-

graphic parameters of the IF do not differ from those of the bulk 2H polytype. The alkali intercalated IF exhibited a *c*-axis expansion of ~4%. Temperature-dependent (4.2–300 K) XRD measurements revealed that the lattice contraction of the IF along the *c* axis upon cooling is similar to that observed for the 2H bulk material.²¹

Single-molecular-layer MoS₂ has been prepared by exfoliation of lithium-intercalated MoS₂ powder in water.^{22–24} The structure of single-layer MoS₂ in aqueous suspension has the octahedral coordination (1T), a structure that does not exist in bulk MoS₂. Furthermore, 1T-MoS₂ was shown to have a metallic character,²⁵ rather than semiconducting 2H polytype. In contrast, XRD and Raman scattering indicate that the single-layer IF-Ws₂ has the trigonal prismatic coordination, similar to that of the bulk 2H structure.

Optical-absorption spectra measurements over the range of 400–800 nm (1.6–3 eV) were carried out on films containing over 80% IF with a 10% size distribution. Standard setup equipped with a tungsten lamp; double-grating monochromator (Jobin-Yvon HRD); liquid-helium cryostat (TBT), and cooled photomultiplier (Hamamatsu RG942) was used. The temperature was varied between 4.2 and 300 K. Careful background subtraction was performed. The accurate position of the *A* and *B* excitons were deduced from the spectra by a Gaussian fitting.

RESULTS

After 3 min annealing of the molybdenum oxide film, the particles of 350±50 Å diameter consist of an oxide core and a few closed sulfide layers (<10), as shown in Fig. 2(a). Subsequent annealing of 90 min leads to a complete conversion of the oxide into an IF-MoS₂ with many layers (>10), as shown in Fig. 2(b). The absorption spectra of the same IF-MoS₂ sample, after 3 and 90 min annealing (sulfidization), are shown in curves 1 and 2 of Fig. 2(c), respectively. They are compared to the spectrum of 2H-MoS₂ bulk at the same temperature (25 K) [curve 3 of Fig. 2(c)]. Figure 2 reveals that the semiconductivity of the layered material is preserved in the IF structures. Nevertheless, after 3 min annealing, the energies of the *A* and *B* excitons are lower by 25 and 80 meV, respectively, compared to the 2H-MoS₂ bulk material. The additional annealing (90 min) did not influence the average size of the IF but added more sulfide layers at the expense of the oxide core. However, the additional annealing leads to a further decrease of the exciton energy: 40 and 100 meV for the *A* and *B* exciton, respectively, compared with the bulk 2H material. A similar redshift of the *A* and *B* exciton energies of IF-MoS₂ has been observed at all studied temperatures (4–300 K). The same trend was observed in the absorption spectra of an IF-Ws₂>1000 Å. After 6 min annealing, in an alcoholic suspension at room temperature, the *A* and *B* excitons are 10 and 30 meV redshifted compared to the 2H bulk and are 1.94 and 2.33 eV, respectively. Further redshifts of 30 and 80 meV for the *A* and *B* excitons, respectively, are observed upon further annealing for 120 min (the *A* and *B* exciton positions are 1.91 and 2.25 eV, respectively). Similar redshifts of the *A* and *B* excitons were observed for all IF-MS₂ samples with more than 6–7 layers at all detected temperatures. This decrease is consistent with

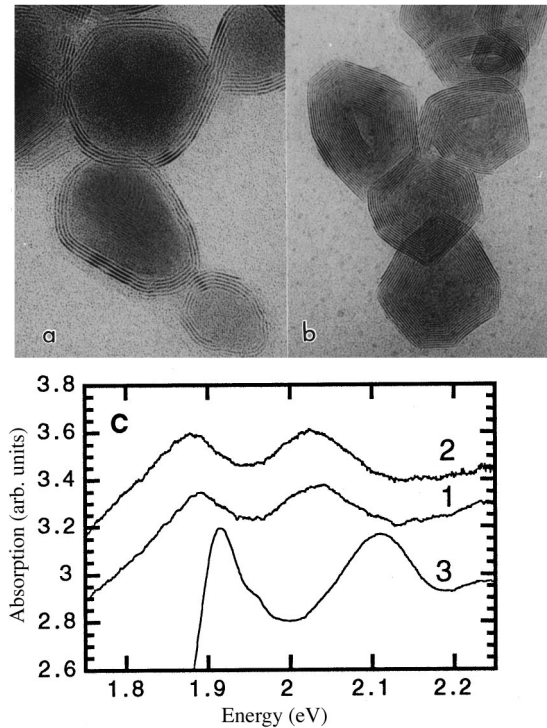


FIG. 2. (a) TEM micrograph of an IF-MoS₂ sample after 3 min annealing. The nanoparticles consist of an oxide core and a few IF layers ($n < 10$). (b) TEM micrograph of the same sample as in (a) after 90 min annealing. The oxide is fully converted into an IF-MoS₂ with many layers ($n > 10$). The distance between two fringes (MoS₂ layers) is 6.2 Å. (c) The absorption spectra at 25 K of the above MoS₂ samples: curves 1 and 2 are of the samples shown in (a) and (b), respectively. Curve 3 is the absorption spectrum of bulk 2H-MoS₂.

the smaller indirect gap measured for a single IF-MoS₂ using STM.⁶ To the best of the authors knowledge, the intrinsic redshift in the absorption spectrum of nanoparticles is unique and was not reported before.

In addition to the redshift of the excitons, a broadening of the peaks and a tailing of the absorption edge to lower energies is observed. These effects may be attributed, at least partially, to the fairly large size and shape distribution of the particles. Whether these effects are intrinsic to the IF particles could be determined when the synthesis of the particles is better controlled and more uniform samples are available.

Understanding the origin of the redshift in IF with $n > 6$ is not straightforward since redshifts are rare in nanometer-size materials. Smaller gaps are generally attributed to sub-band-gap states that emanate from structural imperfections or edge dislocations.²⁶ However, dislocations and impurities are expected to cause a nonsystematic band decrease. Furthermore, the temperature dependence of the exciton energy in IF is similar to that obtained for the excitons in the 2H crystal (see Fig. 3), verifying that the nature of the Wannier excitons is preserved, i.e., the excitons are not bound to dislocations or imperfections. In addition, careful elemental analysis did not reveal impurity levels higher than a few ppm.²⁷ Intercalation of the IF with a few percent of alkali-metal atoms did not produce observable subband-gap states. All these facts indicate that the unique redshift observed in this study is inherent to the topology of the IF structure with many shells.

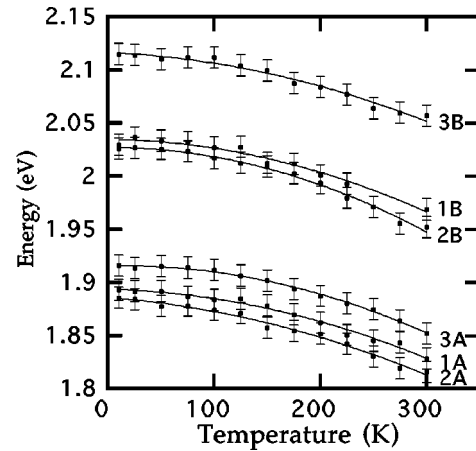


FIG. 3. The temperature dependence (4–300 K) of the A and B excitons of MoS₂ samples shown in Fig. 2. The A and B mark the A and B excitons, respectively: curves 1A and 1B are of the sample shown in Fig. 2(a). Curves 2A and 2B are of the sample shown in Fig. 2(b). Curves 3A and 3B are of the 2H-MoS₂ bulk material. The y-axis error bar is ± 10 meV as determined from Table III.

In order to study the influence of the IF size and number of sulfide layers (n), various IF-MS₂ samples were studied. The absorption spectra of the IF show no dependence of the exciton energies on the size of the IF. Consequently, we conclude that IF with diameters in the range of 150–2000 Å do not exhibit a quantum size effect. Smaller IF (< 80 Å) are likely to exhibit a quantum size effect; unfortunately, they are not available in sufficient quantities for such measurements. A carrier confinement parallel to the layers is not expected, due to the relatively small exciton radius in the xy direction,²⁸ and the (effectively infinite) closed shells of the IF structure. However, we find the IF absorption spectra to be strongly dependent on the number of sulfide layers in an IF. In addition to the already mentioned redshift in the position of the A and B excitons obtained for IF with $n > 6$, a blueshift has been observed for all samples consisting of IF particles with $n < 5$, independent of their diameter. The blueshift of the exciton energies is attributed to a carrier confinement in the direction parallel to the c axis (z direction) similar to the quantum effect observed in MS₂ thin films.¹⁵

It is necessary to estimate the error introduced in the current measurements due to sample inhomogeneity. Fifteen IF samples, 7 IF-MoS₂ and 8 IF-WS₂, are analyzed statistically. The distribution of the number of sulfide layers is determined by TEM for each sample. The positions of the excitons are measured for each sample in the range 4–300 K. The shift in the position of an exciton compared to the 2H bulk is calculated at all detected temperatures. The final shift is determined by averaging the shifts calculated at the different temperatures. Table II includes the distribution of the number of layers (n) and the A and B exciton energy shift of the 15 IF samples (+ blueshift, – redshift, relative to the bulk).

Table II reveals a dependence of the optical spectra of the IF on the number of sulfide layers. Therefore, IF with the same n are expected to exhibit similar energy shifts regardless of their size (diameter). By comparing the shifts obtained for samples with the same n in Table III the error of the energy shift is estimated. From the data presented in Table III, we estimate the total experimental error of the

TABLE II. Diameter and distribution of the number of sulfide layers, as determined by TEM, and the A and B exciton energy shifts for 15 IF samples.

IF Material	IF diameter (Å)	Number of layers (n)	A exciton shift (meV)	B exciton shift (meV)
IF-MoS ₂	2000	5–6	+15	–30
IF-MoS ₂	250	5–10	–25	
IF-MoS ₂	300–400	6–10	–15	–35
IF-MoS ₂	200–400	10–15	–15	–60
IF-MoS ₂	250	15–20	–40	–100
IF-MoS ₂	1000–2000	20–25	–40	–100
IF-MoS ₂	700–800	20–25	–30	–90
IF-WS ₂	175–200	1–2	+50	–10
IF-WS ₂	600–700	1–2	+50	–40
IF-WS ₂	125–150	3–5	+55	+60
IF-WS ₂	200–250	4–6	+50	+10
IF-WS ₂	500–600	5–7	+45	–20
IF-WS ₂	>700	5–8	–25	–25
IF-WS ₂	1500–2000	10–15	–40	–100
IF-WS ₂	>700	10–15	–45	–100

energy shift to be $\leq \pm 10$ meV, of which about 1 meV is an instrumental error while the rest comes from the sample inhomogeneity (size, structure, and distribution of the number of layers).

Figure 4 presents the dependence of the A and B exciton shifts as a function of the IF n for the 15 samples listed in Table II. The x -axis error bar is the distribution of the number of layers determined with the TEM for each sample. The y -axis error bar is ± 10 meV as determined from Table III. Figure 4 suggests a discrimination into four different regimes for the dependence of the energy shift on n . For $n > 10$ a fairly constant redshift is obtained. As mentioned earlier, the redshift is inherent to the topology of the IF structure. IF with $6 < n < 10$ still exhibit a redshift, although this shift decreases with decreasing n . In the regime of $5 < n < 7$ there is a crossover from a redshift to a blueshift. For $n = 1$ or 2, the B exciton is again redshifted.

DISCUSSION

To study the quantum effect in the direction perpendicular to the S - M - S layers, Consadori and Frindt¹⁵ followed the behavior of the A exciton ground-state energy (exciton binding energy ≈ 50 meV), in ultrathin films of 2H-WSe₂ of thickness $13 < L_z < 500$ Å. In the range 80 – 500 Å ($12 < n < 90$), the exciton energy was independent of the film thickness. A linear dependence of the exciton energy on $1/L_z^2$ was

TABLE III. A and B exciton energy shifts of IF samples with a similar number of layers.

IF material	Number of samples	Number of layers (n)	A exciton shift (meV)	B exciton shift (meV)
MoS ₂	2	20–25	-35 ± 5	-95 ± 5
MoS ₂	2	5–10	-20 ± 5	
WS ₂	2	10–15	-42.5 ± 2.5	-100 ± 0

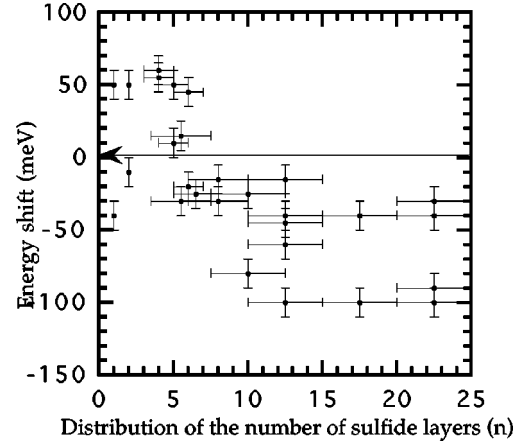


FIG. 4. The dependence of the A and B exciton shifts on the IF n for the 15 samples listed in Table II. The x -axis error bar represents the distribution of the number of layers determined with the TEM for each sample. The y -axis error bar is ± 10 meV as determined from Table III.

found in the thickness range 40 – 70 Å ($6 < n < 11$) attributed to a quantization effect in the z direction:

$$\Delta E_g \approx \frac{\pi^2 \hbar^2}{\mu_{\parallel} L_z^2}, \quad (1)$$

where E_g is the band gap and μ_{\parallel} is the exciton effective mass in the direction parallel to the c axis. For platelets less than 40 Å thick, the shift of the A peak with thickness is much weaker and cannot be accounted for by Eq. (1). Accordingly, in Fig. 5, the A and B exciton energies of IF-MoS₂ and IF-WS₂ are plotted versus $1/L_z^2$ ($L_z = n \times 6.3$ Å) at 25 K. In sharp contrast to the 2H-WSe₂ thin films studied by Consadori and Frindt,¹⁵ here thick films (500 – 1500 Å) consisting of nanoparticles < 1500 Å (IF), but with various “shell” thicknesses are measured. Figure 5 reveals two important results: (1) a linear dependence of the excitons’ energies on $1/L_z^2$ was found also for IF material in the (shell) thickness range 35 – 80 Å ($6 < n < 12, 0.15$

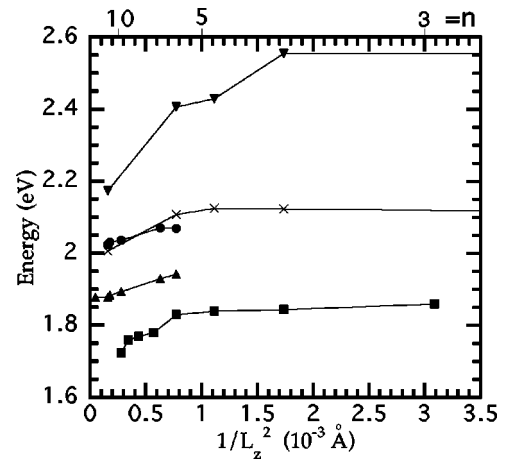


FIG. 5. Plot of the A and B exciton energies of IF-MoS₂ and IF-WS₂ vs $1/L_z^2$. The \blacktriangle and \bullet represent the data for the A and B excitons of IF-MoS₂, respectively; the \times and \blacktriangledown show the data for the A and B excitons of IF-WS₂. The \blacksquare represent the A exciton of 2H-WSe₂ at 77 K (Ref. 15).

$<1000/L_z^2 < 0.75$) similar to that found in thin films. (2) For IF with $L_z > 80 \text{ \AA}$ ($n > 10$), the excitons' energies are thickness independent and saturate at a constant value, which is smaller than the exciton energies obtained for the corresponding single crystals (as mentioned earlier). For IF-MoS₂ (value for 2H in parentheses) at room temperature, the *A* exciton value is 1.82 (1.88) and the *B* exciton value is 1.95 (2.06) eV. For IF-WS₂ at room temperature the *A* exciton position is 1.91 (1.95) and the *B* exciton is shifted to 2.26 (2.36) eV. For both IF-MoS₂ and IF-WS₂, the difference between the *A* exciton energy of the IF and the 2H polytype is smaller than that obtained for the *B* exciton.

Substituting the parameters from the linear part of Fig. 5 into Eq. (1), it is possible to calculate the values of μ_{\parallel}^A and μ_{\parallel}^B . The calculated reduced masses parallel to the *c* axis for IF-MoS₂ at 25 K are $0.92m_0$ and $1.33m_0$, where m_0 is the free-electron mass. These values are smaller than μ_{\parallel}^A and μ_{\parallel}^B of 2H-MoS₂ at 77 K (Refs. 10 and 28) ($\mu_{\parallel}^A = 1.28m_0$ and $\mu_{\parallel}^B = 4.10m_0$). Since the exciton radius is inversely proportional to the exciton mass, the *A* and *B* exciton radii of the IF ‘‘polytype’’ are larger than the corresponding values in the 2H material in the *z* direction ($\parallel c$) and exceed the thickness of a single layer. To calculate the mean reduced masses μ_0^A and μ_0^B of the IF-MoS₂ using the calculated values of μ_{\parallel}^A and μ_{\parallel}^B for IF-MoS₂, Eq. (2) is used:²⁹

$$\frac{1}{\mu_0} = \frac{1}{3} \left(\frac{2}{\mu_{\perp}} + \frac{\varepsilon_{\perp}}{\varepsilon_{\parallel} \mu_{\parallel}} \right), \quad (2)$$

where ε_{\perp} and ε_{\parallel} are the dielectric constants perpendicular and parallel to the *c* axis, respectively. The IF dielectric constants used in the calculation are those of the corresponding bulk material ($\varepsilon_{\perp} = 6.76$ and $\varepsilon_{\parallel} = 2.74$ for 2H-MoS₂).^{29,30} Since there is no quantization in the direction perpendicular to the *c* axis, it is assumed that the values of μ_{\perp}^A and μ_{\perp}^B for the IF-MoS₂ are similar to those of 2H-MoS₂ [$\mu_{\perp}^A = 0.31 m_0$, $\mu_{\perp}^B = 0.99 m_0$ (Ref. 10)]. The calculated mean reduced masses at 25 K for IF-MoS₂ and 2H-MoS₂ (in parentheses) are $\mu_0^A = 0.32 m_0$ ($\mu_0^A = 0.35 m_0$) and $\mu_0^B = 0.75 m_0$ ($\mu_0^B = 1.14 m_0$).³¹ These results indicate that the *B* exciton is more perturbed by the formation of the IF structure than the *A* exciton. Consequently, it is evident that in addition to the shrinkage of the band gap of the IF compared to the 2H polytype, the exciton parameters (reduced mass and radius) are also changed. These results suggest a further investigation into the effect of the curvature on the excitons in layered materials (‘‘bent exciton’’). Such a model has not been discussed theoretically or experimentally in the literature to the best of the authors knowledge.

In correspondence to the observed lattice expansion of $\sim 2\text{--}4\%$ between two adjacent *MS*₂ slabs along the *c* axis, a set of band-structure calculations was done where the distance between adjacent *MS*₂ slabs is increased by 0%, 4%, and 7%. The band structure was calculated by the full potential linear muffin-tin orbitals procedure.³² The influence of the lattice expansion is seen in some band dispersions, but attention is focused on the smallest direct gap at the *K* point, especially the *K*₁ and *K*₄ exciton initial states, as shown in Fig. 6. When the *c* axis expands, a decrease in the splitting of *K*₁ and *K*₄ occurs, until at 7% expansion the two bands

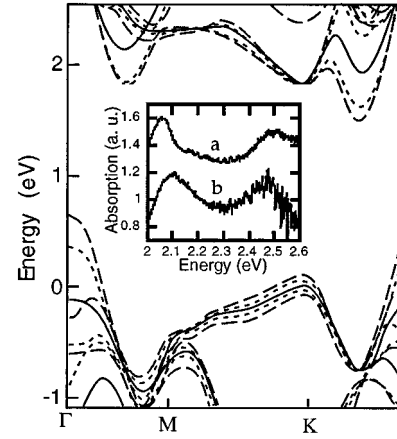


FIG. 6. Electronic band-structure calculation of a set of 2H-MoS₂ where the distance between adjacent *MS*₂ slabs is increased by 0% (---), 4% (-.-), and 7% (—). Inset: Absorption spectra at 25 K of (a) 2H-WS₂ bulk, (b) IF-WS₂, $\sim 700 \text{ \AA}$ diameter, with 1–2 layers.

become degenerate. An expansion of the interlayer (van der Waals) gap by 7% is equivalent to a two-dimensional (2D) single-layer model that becomes evident upon comparing these results with the band-structure calculation for a single S-Mo-S sandwich performed by Kobayashi and Yamauchi,³³ using the linear combination of atomic orbitals method. The convergence of *K*₁ and *K*₄ into one band occurs by lowering the energy of the *K*₄ band (the *A* exciton initial state), and increasing the energy of the *K*₁ band (the *B* exciton initial state). Therefore, this process should come into view as a blueshift of the *A* exciton and a redshift of the *B* exciton, until, for a single layer, the two peaks coincide. Indeed, an increase in the *A* exciton energy and decrease in the *B* exciton energy are observed for three samples consisting of IF or nanotubes with $n = 1$ or 2 as shown in the inset of Fig. 6. Although this increase and decrease of the *A* and *B* exciton energies is observed only when the system approaches a real 2D structure, the interaction between adjacent layers should be taken into account when studying the top of the valence band.

Since the number of atoms in a layer increases with its radius, the layers cannot be fully commensurate. This perturbation of the crystal structure cannot be described by XRD measurements since it is not periodical. A somewhat analogous case exists for 3*R*-MoS₂ where displacement of the adjacent layers leads to a larger unit cell than that of 2H polytype. The 2H and 3*R* polytypes differ in the way the layers are stacked. In the hexagonal (2H) packing the stacking sequence of the layers is *AbA*, *BaB*, ..., while the stacking sequence is *AcA*, *CbC*, *BaB*, ... in the rhombohedral (3*R*) polytype. A comparison of the absorption spectrum of 3*R*-MoS₂ to that of the 2H-MoS₂ shows minor differences, but the *A* and *B* excitons of the former have been shifted to lower energies by 10 and 62 meV, respectively.^{7,34} Note that in analogy to the IF, the redshift of the *B* exciton is substantially greater than the redshift of the *A* exciton (see Fig. 3). Therefore, it is believed that the discommensuration of adjacent layers can be the source of the band-gap shrinkage.

CONCLUSIONS

In conclusion, although IF-MS₂ preserve the semiconductivity of the bulk material even for a single-layer IF, the band

gap is decreased compared to the bulk material. The shrinkage of the gap becomes larger as additional inner layers are formed at the expense of the oxide core, until a saturation value is reached and the gap is no longer affected ($n > 10$). We assign this redshift to the deformations, curvature, and discommensuration between adjacent atomic layers the structure must accommodate in order to form an IF. An increase of the gap is observed in IF consisting of a few sulfide layers. This blueshift is attributed to a quantum confinement in the z direction and is quantitatively described by a model similar to the one used for the absorption spectra of ultrathin platelets of the 2H polytype. Although the studied IF do not

have a single defined structure and size, the unique combination of redshift and blueshift in the absorption spectra is promising both for the study of structure-properties relationship and for tuning the optical properties for specific applications, e.g., for photocatalysis.

ACKNOWLEDGMENT

We wish to acknowledge the support of the Israeli Ministry of Science through the Strategic Materials Research Program and the Minerva Foundation (Munich).

- ¹R. Tenne, L. Margulis, M. Genut, and G. Hodes, *Nature (London)* **360**, 444 (1992).
- ²L. Margulis, G. Salltra, R. Tenne, and M. Tallanker, *Nature (London)* **365**, 114 (1993).
- ³Y. Feldman, E. Wasserman, D. J. Srolovitz, and R. Tenne, *Science* **267**, 222 (1995).
- ⁴Y. Feldman, G. L. Frey, M. Homyonfer, V. Lyakhovitskaya, L. Margulis, H. Cohen, G. Hodes, J. L. Hutchison, and R. Tenne, *J. Am. Chem. Soc.* **118**, 5362 (1996).
- ⁵M. Homyonfer, B. Alpersen, Y. Rosenberg, L. Sapir, H. Cohen, G. Hodes, and R. Tenne, *J. Am. Chem. Soc.* **119**, 2693 (1997).
- ⁶M. Hershinkel, L. A. Gheber, V. Voltera, J. L. Hutchison, L. Margulis, and R. Tenne, *J. Am. Chem. Soc.* **116**, 1914 (1994).
- ⁷J. A. Wilson and A. D. Yoffe, *Adv. Phys.* **18**, 193 (1969).
- ⁸E. Doni and R. Girlanda, in *Physics and Chemistry of Materials with Low-Dimensional Structures*, edited by V. Grasso (Reidel, Dordrecht, 1986), Ser. A, p. 1.
- ⁹R. Coehoorn, C. Haas, J. Dijkstra, and C. J. F. Flipse, *Phys. Rev. B* **35**, 6195 (1987).
- ¹⁰R. Coehoorn, C. Hass, and R. A. de Groot, *Phys. Rev. B* **35**, 6203 (1987).
- ¹¹C. Ballif, P. E. Regula, M. Remskar, R. Sanjinés, and F. Lévy, *Appl. Phys. A: Solids Surf.* **62**, 543 (1996).
- ¹²A. R. Beal, *J. Phys. C* **12**, 881 (1979).
- ¹³J. V. Acrivos, W. Y. Liang, J. A. Wilson, and A. D. Yoffe, *J. Phys. C* **4**, L18 (1971).
- ¹⁴A. D. Yoffe, *Adv. Phys.* **42**, 173 (1993).
- ¹⁵F. Consadori and R. F. Frindt, *Phys. Rev. B* **3**, 4893 (1970).
- ¹⁶B. L. Evans and P. A. Young, *Proc. R. Soc. London, Ser. A* **298**, 7 (1967).
- ¹⁷J. P. Wilcoxon and G. A. Samara, *Phys. Rev. B* **51**, 7299 (1995).
- ¹⁸M. W. Peterson and A. J. Nozik, in *Physics and Chemistry of Materials with Layered Structures*, edited by A. Aruchamy (Kluwer Academic, 1992), Vol. 14, p. 297.
- ¹⁹G. L. Frey, R. Tenne, M. J. Matthews, M. S. Dresselhaus, and G. Dresselhaus (unpublished).
- ²⁰D. J. Srolovitz, S. A. Safran, M. Homyonfer, and R. Tenne, *Phys. Rev. Lett.* **74**, 1779 (1995).
- ²¹F. Kubaneck *et al.* (unpublished).
- ²²P. Joensen, R. F. Frindt, and R. Morrison, *Mater. Res. Bull.* **21**, 457 (1986).
- ²³P. Joensen, E. D. Crozier, N. Alberding, and R. F. Frindt, *J. Phys. C* **20**, 4043 (1987).
- ²⁴D. Yang, S. Jiménez Sandoval, W. M. R. Divigalpitaya, J. C. Irwin, and R. F. Frindt, *Phys. Rev. B* **43**, 12 053 (1991).
- ²⁵D. Yang and R. F. Frindt, *Mol. Cryst. Liq. Cryst. Sci. Technol., Sect. A* **244**, 355 (1994).
- ²⁶K. K. Kam and B. A. Parkinson, *J. Phys. Chem.* **86**, 463 (1982).
- ²⁷M. Homyonfer, Y. Mastai, M. Hershinkel, V. Voltera, J. L. Hutchison, and R. Tenne, *J. Am. Chem. Soc.* **118**, 7804 (1996).
- ²⁸B. L. Evans, in *Physics and Chemistry of Materials with Layered Structures*, edited by P. A. Lee (Reidel, Dordrecht, 1979), Vol. 4, p. 1.
- ²⁹B. L. Evans and P. A. Young, *Phys. Status Solidi* **25**, 417 (1968).
- ³⁰The dielectric constant of the inner IF oxide core is larger, and that of the surrounding air on the outer surface of the IF is smaller than the dielectric constant of the bulk. Therefore, the dielectric constant of the IF is assumed to be similar to that of the corresponding 2H material.
- ³¹The band-gap temperature coefficient dE_g/dT for 2H-MoS₂ and IF-MoS₂ is null up to 75 K, as shown in Fig. 3. This allows the use of the exciton parameters and dielectric constants of 2H-MoS₂ at 77 K in the calculation of exciton parameters at 25 K.
- ³²O. K. Andersen, *Phys. Rev. B* **12**, 3060 (1975).
- ³³K. Kobayashi and J. Yamauchi, *Phys. Rev. B* **51**, 17 085 (1995).
- ³⁴A. Clark and R. H. Williams, *Br. J. Appl. Phys., J. Phys. D* **1**, 1222 (1968).